Assessment of regularization techniques used in solving the ill-posed inverse problem of electrocardiography

Matija Milanič[1], Vojko Jazbinšek[2], Rok Hren[2]

[1]*Institute of Josef Stefan, Ljubljana, Slovenia*
[2]*Institute of Mathematics, Physics and Mechanics, University of Ljubljana, Slovenia*

E-mail: vojko.jazbinsek@imfm.uni-lj.si

Abstract

In this study, we have systematically assessed various regularization techniques which are currently used in solving the ill-posed inverse problem of electrocardiography. For forward computations, we employed an analytical model of the current dipole source placed within the homogeneous isotropic volume conductor consisting of two non-concentric spheres. Analytically calculated potentials on the surface of the larger of the two spheres ("body surface" potentials) served as an input data to recover potentials on the surface of the smaller sphere ("epicardial" potentials). In total, we have examined performance of 10 different regularization techniques in terms of statistical indices (normalized root-mean-square error and correlation coefficient). We have found that the following three regularization methods - first-order Tikhonov (FOT), first-order conjugate gradient (FCG) and first-order least-squares (FLSQR) - most accurately reconstructed "epicardial" potentials, with relative errors between 0.07 and 0.16 (and correlation coefficients between 0,991 and 0,999) depending on a given dipole source location.

1 Introduction

The inverse solution that employs the potential distribution on the epicardial surface as an equivalent source model has been widely studied in electro-cardiography due to its inherent ill-posedness (e.g, [1-4]). A plethora of regularization techniques have been applied to gauge widely oscillating inverse solutions, however, to our knowledge, no systematic comparison among various methodologies exists to date. Here, we employ an analytical model to test the performance of 10 different regularization techniques in reconstructing epicardial potential distributions.

2 Methods

The equivalent potential distribution on the epicardial surface can be found from a known potential distribution on the torso surface by solving generalized Laplace's equation subjected to Cauchy boundary conditions [1-4]. Such a boundary-value problem must be in an arbitrarily shaped volume conductor approximated on a discretized solution domain as the system of linear equations. For the homogeneous and isotropic model of the human torso, this can be achieved by means of the boundary element method, which relates the potentials at the torso nodes (expressed as an m-dimensional vector $\mathbf{\Phi}_B$) to the potentials at the epicardial nodes (expressed as an n-dimensional vector $\mathbf{\Phi}_E$),

$$\mathbf{\Phi}_B = \mathbf{A}\mathbf{\Phi}_E \qquad (1)$$

where $\mathbf{A}$ is the transfer coefficient matrix ($m \times n$) and $n < m$. The transfer coefficient matrix depends entirely on the geometric integrands which can be calculated analytically.

In principle, the epicardial potential distribution could be simply found in the form of a pseudo inverse; however, the matrix $\mathbf{A}$ is ill-conditioned, i.e., its singular values are limiting to zero with particular gap of separation in the singular value spectrum, which yields an unstable solution. A number of approaches have been developed to control the wild oscillations of the solution and the ones we were using in our study are summarized in Table 1.

Table 1. Summary of regularization methods.

Abbr.	Short description	Ref.
ZOT	Zero-order Tikhonov	[6,7]
ZCG	Zero-order Conjugate Gradient	[8]
ZLSQR	Zero-order LSQR	[9]
TSVD	Truncated Singular Value Decomposition	[10]
Nu	ν-method	[10]
FOT	First-order Tikhonov	[11]
FCG	First-order Conjugate Gradient	[8]
FLSQR	First-order LSQR	[9]
TV	Total Variation	[11]
LASSO	Least Absolute Selection and Shrinkage Operator	[12]

The forward solution was computed using a pair of homogeneous and isotropic non-concentric spheres to model the "thoracic" volume conductor and a single current dipole placed inside of the smaller sphere to simulate the current source. Within such a simplified model, the potentials at an arbitrary point can be calculated analytically [5] and for this reason, it is a great tool for comparison of various regularization techniques under well-controlled conditions.

We approximated the thoracic surface by the homogeneous conducting sphere with the unity radius, and the epicardial surface by a smaller sphere with a radius of 0.5, positioned eccentrically (see Figure 1). The body and the epicardial surfaces were tessellated using 1280 and 720 triangles (642 and 362 nodes), respectively. The tessellation of the body surfaces was generated by refinement of icosahedron in four steps and the epicardial surface was generated by refinement of truncated icosahedron in two steps. We put the single dipole in the following 3 locations (see Figure 1):

(i) at an intermediary depth (D1),
(ii) deep within both spheres (D2),
(iii) close to the surfaces of both spheres (D3).

Using 642-node potentials at the surface of the larger sphere ("body surface") with added 40 dB noise, we performed the inverse solutions for 362-node "epicardial" potentials (VE) using the 10 regularization techniques summarized in Table 1. We expressed the accuracy of the inverse solution in terms of the normalized rms (root-mean-square) error (RE) and the correlation coefficient (CC) between the reconstructed and analytically calculated VE_0 on the epicardial surface:

$$RE = \frac{\|VE - VE_0\|_2}{\|VE_0\|_2} \qquad (2)$$

$$CC = \frac{\text{cov}(VE, VE_0)}{\sigma_{VE}\sigma_{VE_0}}, \qquad (3)$$

where cov represents covariance, σ_{VE} and σ_{VE0} standard deviations of VE and VE_0. Results were additionally validated by localizing a single dipole source from

reconstructed 32-leads potential maps using nonlinear Levenberg-Marquardt least square algorithm [13].

3 Results

Figure 2 shows epicardial potential maps for analytical forward solution, zero-order (ZOT) and first-order (FOT) Tikhonov regularizations, and total variation (TV) regularization. In this specific example, the dipole source (D1) was located at an intermediary depth within both spheres. We can clearly see that an optimal inverse solution was obtained by using FOT. The inverse potential map accurately captures all the qualitative features of the corresponding forward map with a small RE of 0.078 and a high CC of 0.9977. Figures 3 and 4 show potential maps for the other two dipoles D2 and D3, respectively.

Tables 2 through 4 summarize our results for all 10 regularization techniques and each of the 3 dipole locations. For each reconstructed potential map, we found the best fitting single dipole source from which we calculated the best fitted map. The following evaluation parameters are presented in tables: (RE_{RA}, RE_{FR}, RE_{FA}) and (CC_{RA}, CC_{FR}, CC_{RA}), i.e. relative errors and correlation coefficients between (reconstructed and analytical, fitted and reconstructed, fitted and analytical) maps, respectively, and localization error Δr, i.e. distance between the fitted and original dipole source location. RE_{RA} and CC_{RA} reflect the quality of reconstructed map, RE_{FR} and CC_{FR} tell how the reconstructed map can be fitted by single dipole, and RE_{FA}, CC_{FA} and Δr give the ultimate answer of how good one can estimate the original dipolar source from epicardial maps inversely calculated from noisy body surface maps.

It is evident from the results in Tables 2-4 that first-order Tikhonov (FOT), first-order conjugate gradient
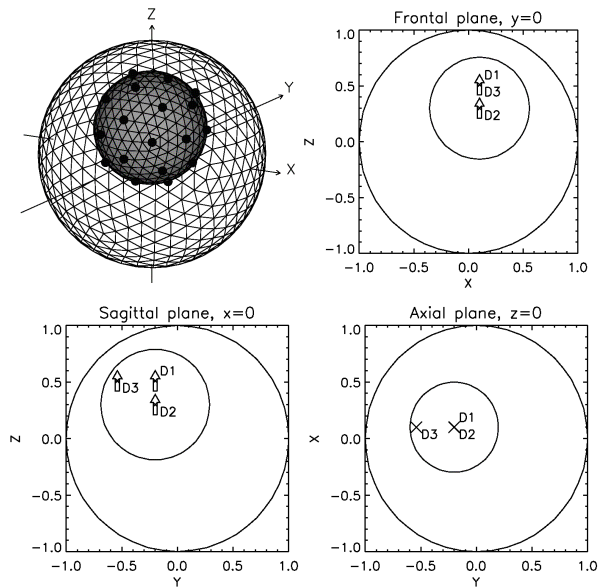

Figure 1. The two-sphere model and 3 cross-sectional views with projections of 3 single dipole sources locations. Bullets on the inner sphere denote 32-leads used in localization.
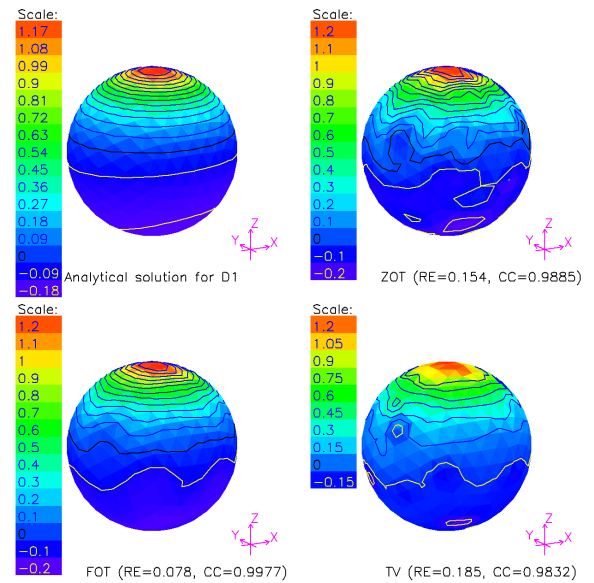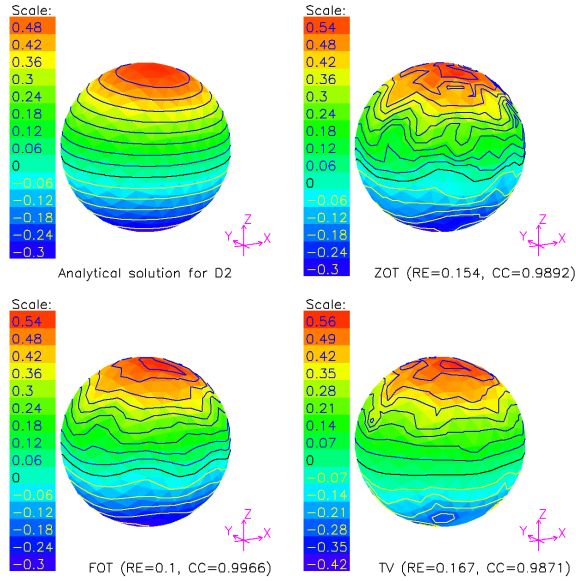

Figure 2. Potential maps on the epicardial surface for D1.

Figure 2. Potential maps on the epicardial surface for D2.

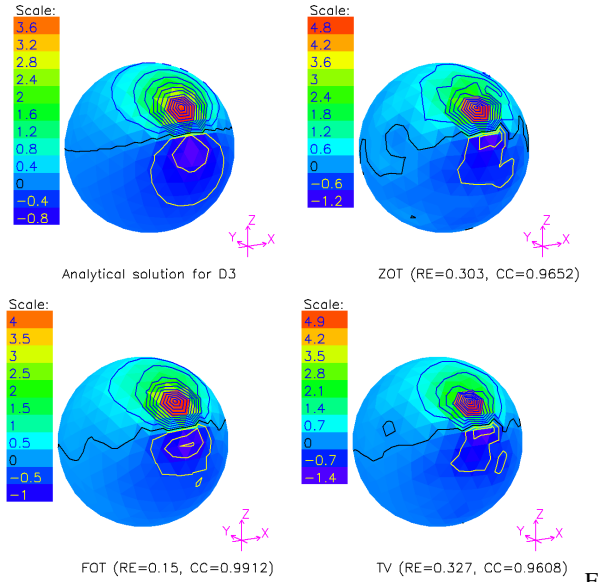Figure 2. Potential maps on the epicardial surface for D3.

Table 2. Results for the dipole source location D1.

Method	RE_{RA}	RE_{FR}	RE_{FA}	CC_{RA}	CC_{FR}	CC_{FA}	Δr
ZOT	0.154	0.142	0.167	0.9885	0.9898	0.9952	0.019
ZCG	0.149	0.141	0.170	0.9892	0.9898	0.9956	0.018
ZLSQR	0.150	0.141	0.170	0.9892	0.9898	0.9956	0.018
TSVD	0.135	0.113	0.159	0.9914	0.9934	0.9972	0.015
Nu	0.150	0.137	0.169	0.9892	0.9904	0.9953	0.018
FOT	0.078	0.070	0.071	0.9977	0.9978	0.9990	0.007
FCG	0.078	0.070	0.071	0.9977	0.9978	0.9989	0.007
FLSQR	0.078	0.070	0.071	0.9977	0.9978	0.9990	0.007
TV	0.185	0.144	0.111	0.9832	0.9892	0.9974	0.015
LASSO	0.148	0.136	0.163	0.9894	0.9907	0.9956	0.018

Table 3. Results for the dipole source location D2.

Method	RE_{RA}	RE_{FR}	RE_{FA}	CC_{RA}	CC_{FR}	CC_{FA}	Δr
ZOT	0.154	0.155	0.140	0.9892	0.9881	0.9963	0.025
ZCG	0.134	0.135	0.128	0.9923	0.9911	0.9981	0.015
ZLSQR	0.151	0.154	0.138	0.9898	0.9881	0.9971	0.020
TSVD	0.132	0.125	0.121	0.9926	0.9923	0.9989	0.009
Nu	0.153	0.153	0.141	0.9894	0.9884	0.9966	0.022
FOT	0.100	0.094	0.068	0.9966	0.9964	0.9987	0.013
FCG	0.100	0.099	0.066	0.9966	0.9959	0.9987	0.013
FLSQR	0.100	0.099	0.066	0.9966	0.9959	0.9987	0.013
TV	0.167	0.138	0.068	0.9871	0.9940	0.9999	0.000
LASSO	0.150	0.152	0.139	0.9898	0.9887	0.9965	0.024

Table 4. Results for the dipole source location D3.

Method	RE_{RA}	RE_{FR}	RE_{FA}	CC_{RA}	CC_{FR}	CC_{FA}	Δr
ZOT	0.303	0.168	0.246	0.9652	0.9862	0.9724	0.016
ZCG	0.331	0.160	0.291	0.9589	0.9874	0.9661	0.012
ZLSQR	0.331	0.160	0.291	0.9588	0.9873	0.9661	0.013
TSVD	0.302	0.152	0.265	0.9657	0.9884	0.9706	0.042
Nu	0.312	0.146	0.274	0.9634	0.9894	0.9690	0.019
FOT	0.150	0.050	0.134	0.9912	0.9988	0.9975	0.010
FCG	0.151	0.049	0.142	0.9910	0.9989	0.9974	0.010
FLSQR	0.151	0.049	0.141	0.9910	0.9989	0.9974	0.010
TV	0.327	0.096	0.364	0.9608	0.9956	0.9462	0.017
LASSO	0.314	0.182	0.253	0.9627	0.9837	0.9711	0.018

(FCG) and first-order least-squares (FLSQR) most accurately reconstructed "epicardial" potentials, i.e. the smallest RE_{RA} and the highest CC_{RA}, irrespective of dipole location. Results also showed that the worst reconstructions were obtained for the source originated near both the epicardial and body surfaces (D3). In this case, the potential map changed rapidly across the surface area near the source, which probably affected the accuracy due to a finite dimension of triangles on the tessellated surfaces. The average distances between triangle nodes were 0.1 with a range from 0.087 to 0.105 and 0.15 with a range of 0.138 to 0.165 for the epicardial and body surface, respectively. Results for the deeper source (D2) showed that first order Tikhonov regularizations (FOT, FCG and FLSQR) still gave the best reconstruction but not so markedly better than others, which was the case for the other two dipole locations. The extrema of potential maps from deeper sources are much smaller than the extrema of maps from sources nearer the surface. The reconstructed maps for such sources are therefore more affected by the added noise.

Comparison of fitted and analytically calculated maps (RE_{FA} and CC_{FA}), and localization error (Δr) in Tables 2-4 again showed that the best figures were obtained when the maps reconstructed by the first-order Tikhonov regularizations were used in the fitting procedure ($\Delta r < 0.013$ and $CC_{FA} > 0.997$ for all three dipoles). There was only one exception, i.e. for the D2 dipole we got a perfect localization ($\Delta r < 0.0005$) and correlation ($CC_{FA}=0.9999$) with the TV method.

4 Discussion

The main finding of our study is that 3 regularization methods performed substantially better than the other 7 techniques. The main reason for the difference in performance is that methods FOT, FCG, and FLSQR all use first-order penalty function, which may better approximate quickly changing areas of epicardial potentials than, for example, the zero-order ones. Recently, Gosh and Rudy [4] noted that TV method (also called L1 regularization) may better capture spatial pattern of epicardial potentials than techniques, which minimize the square of the norm. In our study, that is, with our model of the source and volume conductor, performance of the TV method was consistently inferior to the performances of FOT, FCG, and FLSQR methods. Future work would be needed to better elucidate this point.

References

[1] H.S. Oster, B. Taccardi, R.L. Lux, P.R. Ershler, Y. Rudy. Noninvasive electrocardiographic imaging: Reconstruction of epicardial potentials, electrograms, isochrones and localization of single and multiple electrocardiac events. Circulation **96:** 1012-1024, 1997.

[2] Y. Rudy, B.J. Messinger-Rapport. The inverse problem in electrocardiography: Solutions in terms of epicardial potentials. Crit. Rev. Biomed. Eng. **16**: 215-268, 1988.

[3] R. Hren. Value of epicardial potential maps in localizing pre-excitation sites for radiofrequency ablation. A simulation study. Phys. Med. Biol. **43**:1449-1468, 1998.

[4] S. Gosh, Y. Rudy. Application of L1-norm regularization to epicardial potential solution of the inverse electrocardiography problem. Ann. Biomed. Eng. **37**: 902-912, 2009.

[5] D. Yao. Electric Potential Produced by a Dipole in a Homogeneous Conducting Sphere, IEEE Trans. Biomed. Eng. **44**: 964-966, 1999.

[6] A. Tikhonov, V. Arsenin. Solution of Ill-Posed Problems. Washington, DC: Winston, 1977.

[7] D.H. Brooks, F.A. Ghandi, R.S. MacLeod. Inverse Electrocardiography by Simultaneous Imposition of Multiple Constraints, IEEE Trans. Biomed. Eng. **46**: 3-18, 1999.

[8] M. Hanke. Conjugate Gradient Type Methods for Ill-Posed Problems. Harlow: Longman Scientific & Technical, 1995.

[9] C.C. Paige, M.A. Saunders. LSQR: An algorithm for sparse linear equations and sparse least squares, ACM Transactions on Mathematical Software **8**: 43-71, 1982.

[10] P.C. Hansen. Rank-Deficient and Discrete Ill-Posed Problems. Philadelphia: SIAM, 1998.

[11] G. Subham, Y. Rudy. Application of L1-Norm Regularization to Epicardial Potential Solution of the Inverse Electrocardiography Problem, Annals Biomed. Eng. **37**: 902-912, 2009.

[12] M. Schmidt. Least Squares Optimization with L1-Norm Regularization, Project Report, University of British Columbia, 2005.

[13] W.H. Press, B.P. Flannery, S.A. Teukolsky,W.T. Vetterling. Numerical Recipes - The Art of Scientific Computing, Cambridge University Press, 1989.